

# In medium pp cross section with screened OBE interaction in relativistic nuclear matter

J. Diaz-Alonso\*, L. Mornas†

\*DARC, UPR 176 CNRS, Observatoire de Paris - Meudon, F-92195 Meudon, France  
and Universidad de Oviedo, Departamento de Física, E-33007 Oviedo, Spain

†Departamento de Física Teórica, Universidad de Valencia, 46100 Burjasot (Valencia), Spain

February 16, 2019

PACS: 25.40.Cm, 21.30.-x, 21.65+f, 24.10.Jv, 21.60.Jz

keywords: in-medium NN cross section, screened one-boson exchange, relativistic RPA, zero-sound

## Abstract

We investigate the modification induced on the nucleon-nucleon cross section by screening of the interaction inside nuclear matter. The interaction is described by the relativistic one boson exchange of  $\sigma$ ,  $\omega$  and  $\pi$  mesons. Medium effects enter as loop corrections to the meson propagators and are characterized not only by density, but also by temperature and velocity with respect to the center of mass of the collision. The cross section displays peaks for some specific values of the velocity, corresponding to the excitation of zero-sound modes of the longitudinal  $\omega$  field. The enhancement factor amounts to about 1.5 under reasonable conditions and goes up to  $10^3$  in some extreme cases. It increases with density and is reduced at finite temperature. These findings may have verifiable consequences on the angular dependence of the measurable secondary particle distributions.

## 1 Introduction

Dissipative effects play an important role in explaining the shapes of the angular distributions and energy spectra of the secondary particles produced in a relativistic heavy ion collision. For this reason, the cross section is an important ingredient in all kinds of numerical simulations of these collisions, be it in the molecular dynamics approach [1, 2], kinetic theory approaches like the Boltzmann-Uehling-Uhlenbeck equation [3, 4], or the hydrodynamical models where it enters through the transport coefficients [5]. Early calculations used a constant value of the cross section  $\sigma=40$  mb or fits to the measured free value like that provided by Cugnon *et al.* [6]. It has become obvious however that this does not well reproduce the available experimental data. Rather than ascribing all the discrepancies between data and numerical simulations to an excessive stiffness of the equation of state, which anyway would be incompatible with other data, it has soon been recognized that the medium may affect the nucleon-nucleon cross section by modifying the strength of the interaction and the available phase space. Actually, a reduction of the cross section by a factor of 20 % would be necessary to explain the latest BUU, RQMD and AMD simulations [1, 2, 3, 4]. The accuracy of the calculations have now come to a point where they can be used to set constraints on the in-medium cross section. Experimental observables like transverse flow and balance energy

seem to be useful in this respect. This in turn calls for an improvement of the theoretical insight on the medium dependence of the nucleon-nucleon cross section.

Several attempts to calculate medium corrections to the cross section already exist. The first point to precise is in what type of background matter does the collision take place. Some authors like Faessler *et al.* [7] or Fuchs *et al.* [8] consider that the background consists of a momentum distribution in two well separated Fermi spheres. This corresponds to the initial stage of a heavy ion collision and is far out of equilibrium. Other authors like Machleidt *et al.* [9] or Alm *et al.* [10] consider that the background is nuclear matter, supposedly of infinite extension, and not far from equilibrium. This rather corresponds to the intermediate stage of the heavy ion collision after a fireball was formed. This latter case is what we are interested in here.

Medium effects enter at several levels of the calculation of the cross section. Older evaluations only took into account what happens if the nuclear mass is shifted to an effective smaller value inside nuclear matter. Then, in the last few years were performed a number of calculations with the Brueckner formalism [9, 10, 11]. In this approach, an infinite series of ladder diagrams are resummed. The nucleon propagators, *i.e.* the uprights of the ladder, are dressed. The medium effects enter as Pauli blocking factors on the intermediate states in the inner nucleon lines. The meson lines are the free ones, corresponding to an unscreened interaction.

On the other hand, we would like to discuss in this letter the influence of the screening of the interaction by the surrounding nuclear matter. In a model where the nucleon-nucleon interaction is described by relativistic meson exchanges, we take into account the dressing of the meson lines in the first Born approximation. We restrict ourselves here to proton-proton or neutron-neutron scattering since, in this case, we can reproduce the available data to a satisfactory level of accuracy with the exchange of  $\sigma$ ,  $\omega$  and  $\pi$  mesons only, which makes the interpretation of the results more transparent.

The study of the effects of the medium have been concentrated up to now on the density dependence, but do not in general take into account the temperature dependence or the effects of the motion of the center of mass of the colliding particles with respect to the nuclear plasma in which it takes place (see however Alm *et al.* [10]). We will address these three points here. A detailed study of the density and temperature dependence of the total and differential elastic  $p$ - $p$  cross section was performed in our first paper [12] (hereafter referred to as paper I). We will recall here the main results and refer the reader to [12] for details. In paper I, it was assumed that the background nuclear matter was at rest with respect to the center of mass of the collision. This assumption is released here.

## 2 The model

We are working with the standard quantum hadrodynamics lagrangian with  $\sigma$ ,  $\omega$  and  $\pi$  meson exchange (see *e.g.* [13]). As mentioned above, this is the minimal model which permits to reproduce the available experimental data on  $p$ - $p$  scattering to a satisfactory level of accuracy. The interaction lagrangian reads

$$\mathcal{L} = g_\sigma \bar{\psi} \sigma \psi + g_\omega \bar{\psi} \gamma^\mu \omega_\mu \psi + g_\pi \bar{\psi} \gamma^5 \vec{\tau} \vec{\pi} \psi \quad (1)$$

The differential elastic cross section was calculated in the Born approximation. In the center of mass of the collision,

$$d\sigma/d\Omega = 1/(64\pi^2 s) |\mathcal{M}|^2 \quad (2)$$

where  $s$  is the Mandelstam variable  $s = 4E_{c.m.}^2$  and the transition matrix is given in condensed form by

$$\mathcal{M} = \sum_{m,n=\sigma,\omega,\pi} (\bar{U}_3 \Gamma_m U_1) G_{31}^{mn} (\bar{U}_4 \Gamma_n U_2) - \text{exchange} \quad (3)$$

In this expression the  $U$ 's are the spinors defining the incoming ( $U_1, U_2$ ) and outgoing ( $U_3, U_4$ ) nucleon states. The indices  $i = 1, 2, 3, 4$  carried by the spinors stand for the momenta  $p_i^\mu$  and the spin-isospin quantum numbers  $s_i, t_i$ .  $G_{31}^{mn}$  is the propagator matrix which depends on the momentum transfer  $k_{31}^\mu = p_1^\mu - p_3^\mu$ . In free space, it reduces to the standard form

$$G_{31}^{mn} = \text{Diag} \left( \frac{-i[g^{\mu\nu} - \frac{k^\mu k^\nu}{k^2}]}{k^2 - m_\omega^2}, \frac{i}{k^2 - m_\sigma^2}, \frac{i}{k^2 - m_\pi^2} \right) \quad (4)$$

$\Gamma$  is the coupling matrix defined by

$$\Gamma = \begin{pmatrix} -ig_\omega \gamma^\mu \\ ig_\sigma \\ g_\pi \gamma_5 \vec{\tau} \end{pmatrix} \quad (5)$$

In the explicit calculation of the transition matrix from these formulae, all the coupling constants in  $G^{mn}$  and  $\Gamma_m$  are to be multiplied by the corresponding form factors  $\mathcal{F}_m(k) = (\Lambda_m^2 - m_m^2)/(\Lambda_m^2 - k^2)$ . The exchange term is obtained by interverting the indices 3 and 4. In the following we consider only the spin-averaged cross section obtained by replacing  $|\mathcal{M}|^2$  by  $|\overline{\mathcal{M}}|^2 = (1/4) \sum_{s_i} |\mathcal{M}|^2$ . We obtain the  $p$ - $p$  cross-section for the isospin quantum numbers  $t_1 = t_2 = t_3 = t_4 = 1$  and the  $n$ - $n$  cross section for  $t_1 = t_2 = t_3 = t_4 = 0$ .  $\sigma_{pp}$  and  $\sigma_{nn}$  are equal in our approximation where the Coulomb interaction was subtracted and the neutron and proton masses are the same.

In paper I we performed a fit of the free elastic  $p$ - $p$  cross section using the available experimental data [14]. We kept constant the masses of the mesons and the pion-nucleon coupling ( $m_\sigma=550$  MeV,  $m_\omega=783$  MeV,  $m_\pi=550$  MeV,  $g_\pi^2/(4\pi)=14.4$ ) and fitted the coupling constants  $g_\sigma, g_\omega$  and the cutoffs  $\Lambda_\sigma, \Lambda_\omega, \Lambda_\pi$ . Several sets of parameters were found to reproduce the data to a satisfactory level of accuracy. It was checked that the in-medium behavior of the cross section was the same for all choices of the parameter set. The calculations are performed here with parameter set A of paper I:  $g_\sigma = 3.80$ ,  $g_\omega = 9.31$ ,  $\Lambda_\sigma = 1298.8$ ,  $\Lambda_\omega = 1240.5$ ,  $\Lambda_\pi = 362.1$ .

Inside the medium, the momenta and masses of the incoming and outgoing nucleons must be replaced by their effective counterparts. In the Hartree approximation,  $p_i^\mu \rightarrow (p_i^\mu)^* = p_i^\mu - g_\omega <\omega^\mu>$ ,  $m \rightarrow m_* = m - g_\sigma <\sigma>$ .

The propagator matrix must also be modified in order to take into account that the N-N interaction is mediated by dressed mesons. The dispersion relations and propagators of the mesons at finite temperature were obtained from a linear kinetic analysis of perturbations around the Hartree ground state, starting from the relativistic quantum B.B.G.K.Y. hierarchy [15]. The results of this method coincide at  $T=0$  with those of the one-loop approximation [16]. The calculation takes into account renormalized vacuum polarization contributions which are crucial in obtaining a physically reasonable behavior of the propagation modes [15].

The propagator matrix so obtained has the form [12, 16, 17].

$$G^{mn} = \begin{pmatrix} G_\omega^{\mu\nu} & G_{\sigma\omega}^\mu & 0 \\ G_{\omega\sigma}^\mu & G_\sigma & 0 \\ 0 & 0 & G_\pi \end{pmatrix} \quad (6)$$

with

$$\begin{aligned}
G_\sigma &= i \frac{k^2 - m_\omega^2 + g_\omega^2 \Pi_{\omega L}}{D_{\sigma-\omega L}(k)} \\
G_\omega^{\mu\nu} &= -i \left[ \mathcal{T}^{\mu\nu} \frac{1}{k^2 - m_\omega^2 + g_\omega^2 \Pi_{\omega T}} + \Lambda^{\mu\nu} \frac{k^2 - m_\sigma^2 + g_\sigma^2 \Pi_\sigma}{D_{\sigma-\omega L}(k)} - \frac{k^\mu k^\nu}{m_\omega^2 k^2} \right] \\
G_{\sigma\omega}^\mu &= -i \eta^\mu \frac{g_\sigma g_\omega \Pi_\times}{D_{\sigma-\omega L}(k)} \\
G_\pi &= i \frac{1}{k^2 - m_\pi^2 + g_\pi^2 \Pi_\pi}
\end{aligned} \tag{7}$$

The denominator of the  $\sigma$ , longitudinal part of the  $\omega$  and mixing propagators is given by the mixed  $\sigma$ - $\omega$  dispersion relation

$$D_{\sigma-\omega L}(k) = (k^2 - m_\sigma^2 + g_\sigma^2 \Pi_\sigma)(k^2 - m_\omega^2 + g_\omega^2 \Pi_{\omega L}) + g_\sigma g_\omega \Pi_\times^2 \tag{8}$$

In these expressions we defined the auxiliary quadrivector  $\eta^\mu$  and the projectors onto the longitudinal ( $\Lambda^{\mu\nu}$ ) and transverse ( $\mathcal{T}^{\mu\nu}$ ) modes as functions of the 4-velocity  $u^\mu$  of the fluid as follows:

$$\begin{aligned}
\eta^\mu &= u^\mu - \frac{k \cdot u}{k^2} k^\mu & ; & & \tilde{g}^{\mu\nu} &= g^{\mu\nu} - \frac{k^\mu k^\nu}{k^2} \\
\mathcal{T}^{\mu\nu} &= \tilde{g}^{\mu\nu} - \frac{\eta^\mu \eta^\nu}{\eta^2} & ; & & \Lambda^{\mu\nu} &= \frac{\eta^\mu \eta^\nu}{\eta^2}
\end{aligned} \tag{9}$$

The polarizations  $\Pi(k)$  of the meson fields are functions of the thermodynamical state (density and temperature) of the matter and on the transferred 4-momentum  $k^\mu = (\omega, \vec{q})$ . There is a mixing between the  $\sigma$  and longitudinal- $\omega$  propagation modes. The  $\pi$  propagation is decoupled from the dynamics of the other mesons in symmetric nuclear matter. We use the notation

$$\Pi_\times = \eta_\mu \Pi_{\sigma\omega}^\mu \quad ; \quad \Pi_{\omega L} = -\Lambda_{\mu\nu} \Pi_\omega^{\mu\nu} \quad ; \quad \Pi_{\omega T} = -\mathcal{T}_{\mu\nu} \Pi_\omega^{\mu\nu} / 2 \tag{10}$$

for the mixing, longitudinal and transverse parts.

The polarizations are complex. In the  $T = 0$  limit, the imaginary part of the polarizations vanish outside the region defined by

$$\sqrt{(p_F - q)^2 + m_*^2} - \sqrt{p_F^2 + m_*^2} < \omega < \sqrt{(p_F + q)^2 + m_*^2} - \sqrt{p_F^2 + m_*^2} \tag{11}$$

(where  $p_F$  is the Fermi momentum and  $m_*$  the effective mass of the nucleon inside the medium). Inside this region, the propagation modes are damped by the decay into particle-hole pairs. At finite temperature the imaginary parts are finite for any space-like mode.

The dependence on the velocity of the medium comes through the quadrivector  $\eta^\mu$ . In the referential (R1) where the fluid is at rest,  $u^\mu = (1, \vec{0})$  and the momentum transfer is  $k^\mu = (\omega, \vec{q})$

In the center of mass of the collision (referential (R2)), the background fluid moves with a velocity  $u^\mu = (\gamma, \gamma \vec{v})$  parametrized by

$$\vec{v} = \begin{pmatrix} v \sin \alpha \sin \varphi \\ v \sin \alpha \cos \varphi \\ v \cos \alpha \end{pmatrix} \tag{12}$$

The momentum transfers for the direct ( $k_{31}$ ) and exchange ( $k_{41}$ ) diagrams are

$$k_{31}^\mu = (0, 0, p \sin \theta, p(1 - \cos \theta)) \quad ; \quad k_{41}^\mu = (0, 0, -p \sin \theta, p(1 + \cos \theta)) \tag{13}$$

with  $p = \sqrt{E_{c.m.}^2 + m_*^2}$  and  $\theta$  is the *c.m.* scattering angle.

One goes from (R1) to (R2) by performing a boost of four-velocity  $(\gamma, \gamma\vec{v})$  and a rotation. In the referential (R1),

$$\begin{aligned} k_{31}^\mu(R1) &= (\omega_\ominus, \vec{q}_\ominus) \quad ; \quad k_{41}^\mu(R1) = (\omega_\oplus, \vec{q}_\oplus) \\ \omega_{(\ominus)} &= \gamma v p [\pm \sin \alpha \cos \varphi \sin \theta - \cos \alpha (1 \mp \cos \theta)] \\ q_{(\ominus)} &= [\omega_{(\ominus)}^2 + 2p^2 (1 \mp \cos \theta)]^{1/2} \end{aligned} \quad (14)$$

### 3 In medium cross section for vanishing relative velocity

When the rest frame of the background nuclear matter coincides with the center of mass of the colliding particles, *i.e.* when (R1)  $\equiv$  (R2), we only need purely spacelike momentum transfer  $k^\mu = (0, \vec{q})$  for the calculation of the polarizations (*cf.* Eq. (14)). Moreover the transverse projector  $\mathcal{T}^{\mu\nu}$  equals  $Diag(0, -1, -1, -1)$  and the longitudinal one  $\Lambda^{\mu\nu}$  has only one non-vanishing component  $\Lambda^{00} = 1$ .

Our results at finite density and temperature are summarized in Fig. 1. In this figure, the diamonds represent experimental data points for the total elastic *p-p* cross section in vacuum and the full line is our best fit obtained in paper I. With the same parameter set are plotted the cross section for density  $n = 0.1 n_0$  (dot-dashed line),  $n = n_0$  (dashed line) and  $n = 4 n_0$  (dotted line). The curves are labelled with temperature; the thickness of the lines increases with T.

When the density is increased at zero temperature, the cross section is reduced. The reduction factor is larger in the low energy range, so that we obtain that the in-medium elastic *p-p* cross section becomes nearly independent of the energy of the incident particles at normal nuclear density  $n = n_0$ , with a value  $\sigma_{pp}(T = 0, n = n_0) = 18$  mb. Further increasing the density above  $n = 2 n_0$  leaves the in-medium cross section unchanged at  $\sigma_{pp}(T = 0, n = 2 n_0) = 17$  mb. The behaviour with temperature is non monotonous. Increasing the temperature first slightly increases the cross section. For example, we have  $\sigma_{pp}(T = 100, n = n_0) \simeq 21$  mb. For very high temperatures, the cross section decreases again. At  $T = 250$  MeV, we have  $\sigma_{pp}(T = 250) \simeq 16.5$  mb for any value of energy or density. Temperature dependence is less pronounced than density dependence and the amplitude of variations with temperature is largest for densities  $n \simeq n_0$ .

When performing the fit, we could also reproduce to some extent the experimental data for the differential *p-p* cross section [12]. The fit was only qualitative at low energies and upgraded to quantitative at high energies above  $\sim 600$  MeV. With this restriction in mind, our model predicts that high densities favour forward/backwards peaking.

The behaviour with density can be understood from that of the polarizations. At zero temperature, the propagators of the mesons are strongly affected by particle/hole production below a threshold value of the momentum transfer  $q = 2p_F$ . In particular,  $\sigma$ - $\omega$  mixing is very efficient in this range since, for example, a  $\sigma$  meson may decay into a virtual particle/hole pair and recombine as a longitudinally polarized  $\omega$  meson. Above this threshold, Pauli blocking forbids particle/hole formation and mixing. Similarly to what occurs for the *N-N* potential, the cross section results from a delicate cancellation between the scalar and vector contributions. As density and the Fermi momentum  $p_F$  increase, the mixing perturbs the balance between these terms for *c.m.* energies and scattering angles fulfilling the condition  $q = \sqrt{2(E_{c.m.}^2 - m_*^2)(1 \pm \cos \theta)} < 2p_F$ , resulting in the observed behaviour. At finite temperature, the Fermi distribution functions are smooth and phase-space opens for mixing above the

threshold  $q = 2p_F$  as well. Moreover, particle/hole formation is easier at high temperature since the effective mass of the nucleon decreases with  $T$ .

Experimental constraints begin to be available from the latest simulations of heavy ion collisions by BUU [3, 4], RQMD [1] or AMD [2] codes. New experimental observables are being defined and their accurate measurement is rendered possible by the new generation of  $4\pi$  detectors. In particular, one defines the balance energy  $E_{bal}$  as the beam energy for which the transverse flow vanishes. It is argued [18] that  $E_{bal}$  does not depend on the stiffness of the equation of state and is nearly exclusively sensitive to the cross section. This feature permitted Klakow *et al.* [4] to conclude that the cross section was reduced by a factor  $\sim 20\%$  in a BUU simulation of  $A+A$  collisions at 200 MeV/A. Another approach is to perform molecular dynamics simulations with a density-dependent cross section. The RQMD simulation of Khoa *et al.* concluded similarly to a reduced in-medium cross section from a study of the stopping power. Up to our knowledge, the most precise constraints were obtained by Tanaka, Horiuchi and Ono [19] from a simulation of  $p + {}^{40}\text{Ca}$  collisions with the AMD code.

We checked that our results are compatible with these constraints and that we obtain a similar overall dependence of the in-medium cross-section as the one extracted by Tanaka *et al.*. At  $T=0$ , we somewhat overpredict the reduction factor at high beam energies. Finite temperature effects were seen to improve the agreement. As a matter of fact, some thermal energy is expected to be released from the conversion of collision energy of the incident proton.

## 4 In medium cross section for finite relative velocity

The velocity of the background nuclear matter enters the expression of the cross section through the meson propagators. There is an explicit dependence coming from the projectors  $\Lambda^{\mu\nu}$ ,  $\mathcal{T}^{\mu\nu}$  (see Eq. (9)). The projectors act by attributing velocity-dependent weights to the various components of the currents  $\mathcal{J}$  like *e.g.*  $\mathcal{J}_\omega^{\mu\nu} = (\bar{U}_3\gamma^\mu U_1)(\bar{U}_4\gamma^\nu U_2)$ . There is also an indirect dependence in the velocity in the expression of the polarizations  $\Pi(\omega_{(\oplus)}, q_{(\oplus)})$  coming from the boost transformation Eq. (14). In contrast to the zero velocity case where the momentum transfer  $k^\mu$  entering the expression of the polarizations was confined to the axis  $\omega=0$ ,  $k^\mu = (\omega_{(\oplus)}, q_{(\oplus)})$  now spans all the spacelike region.

We split for convenience the discussion in three cases, namely (i)  $v = (0, 0, v_z)$  when the velocity is parallel to the axis of the incident particles in the center of mass frame of the collision, (ii)  $v = (0, v_y, 0)$  when the velocity is in the reaction plane and perpendicular to the axis of the incident particles, and (iii)  $v = (v_x, 0, 0)$  when the velocity is perpendicular to the reaction plane. Let us first give a summary of the most salient features of the results before we go to the interpretation.

For moderate values of the velocity along the axis defined by the incident particles ( $v = v_z$ ), the cross section is slightly enhanced at low densities and reduced at high densities. When some temperature is introduced, the low density enhancement disappears and the high density reduction persists. At highly relativistic  $v_z$  velocities ( $\gamma_z \gtrsim 5$ ), the cross section displays a series of peaks, of which three are clearly visible. The height of the peaks increases with density. The effect of finite temperature is to gradually wash out these peaks. The peaks are superposed on an additional increase of the cross section, which stabilizes to a large constant value for large  $\gamma_z$ . This additional enhancement persists when introducing finite temperature.

For low values of the velocity inside the reaction plane and orthogonal to the beam axis ( $v = v_y$ ), the cross section is first approximately constant for densities up to  $n = n_0$  and somewhat reduced at high density when increasing  $v_y$ . Further increasing  $v_y$ , one meets a peak

structure (see Fig. 2) superposed on a smooth increase similar to the one already observed in the case  $v = v_z$ , but occurring for more physical values of the velocity. There is first a very sharp peak for a characteristic value  $\hat{v}_y$  immediately followed by one or two smoother peaks. Further increasing the velocity, the cross section slowly decreases and stabilizes to a constant value  $\sigma_{med}/\sigma_{free}(v_y \rightarrow c)$  somewhat larger than  $\sigma_{med}/\sigma_{free}(v = 0)$  and approximately equal to 1. We were able to check that the peak structure originates from the velocity dependence of the polarizations while the residual temperature-independent enhancement at  $v_y \rightarrow c$  is due to the velocity dependence of the projectors  $\Lambda^{\mu\nu}$ ,  $\mathcal{T}^{\mu\nu}$ . The same holds for the case  $v//z$ .

The characteristic velocity  $\hat{v}_y$  at which the sharp peak takes place is density dependent, *e.g.* one has  $\hat{v}_y \simeq 0.41c$  for  $n = n_0$  and  $\hat{v}_y \simeq 0.57c$  for  $n = 2n_0$  (see Fig. 2a). The height of the peak increases with increasing density and is reduced by increasing the temperature (see Fig. 2b). At  $T = 10$  MeV, a broad bump is still clearly visible around  $\hat{v}_y$ , at high temperature  $T \gtrsim 50 - 100$  MeV it has completely disappeared.

No appreciable modification is observed for velocities orthogonal to the reaction plane ( $v = v_x$ ) up to  $v_x \simeq 0.8c$ . On the other hand, the total cross section starts to increase above this value and continues to grow indefinitely as  $\gamma_x \rightarrow \infty$ .

The angular dependence of the differential cross section deviates appreciably from its behavior when the fluid is at rest. For each value of the velocity, there is a favoured angle, but this effect is most appreciable for small angles, so that finite velocities also contribute to make the cross section more forward/backward peaked with respect to its vacuum value.

We concentrate on the behaviour with  $v_y$  as it illustrates the other cases. Moreover this is the case most liable to lead to observable consequences since the peaks appear for reasonable values of the relative velocity. The peak structure is to be related to the excitation of the zero sound modes. These modes arise from the mixed  $\sigma$  - longitudinal  $\omega$  part of the dispersion relation; they were studied in previous work [15, 17]. A contour plot of the mixed dispersion relation  $D_{\sigma-\omega L}(\omega, q)$  in the  $q - \omega$  plane of transferred momentum is shown in Fig. 3 for  $T = 0$ ,  $n = n_0$ . The level  $D_{\sigma-\omega L}(\omega, q) = 0$  gives the location of the zero-sound branch. For not too high values of the energy-momentum transfer, the region of the zero sound branches can be crossed for some values of the velocity in the medium: If  $(\omega, q)$  coincides with a zero-sound solution  $k_{zs}^\mu = (\omega_{zs}, q_{zs})$  of the dispersion relation  $D_{\sigma-\omega L}(k_{zs}^\mu) = 0$ , there will be a critical value of the relative velocity  $\hat{v}$  solution of

$$\omega_{zs} = \omega_{(\ominus)} = \gamma \hat{v} p [\pm \sin \alpha \cos \varphi \sin \theta - \cos \alpha (1 \mp \cos \theta)] \quad (15)$$

(*cf.* Eqs. (8) and (14)) for which the real part of the dispersion relation vanishes. Since the dispersion relation appears in the denominator of the propagators (see Eq. (8)), a pole appears in the expression of the cross section (see Eqs. (2) and (3)) if the imaginary part of  $D_{\sigma-\omega L}$  vanishes as well. For relative velocities near  $v_{crit}$ ,  $D_{\sigma-\omega L}$  is still reduced and as a consequence, the cross section enhanced.

For example, at  $n = n_0$  and  $T=0$ , we have drawn on Fig. 3 the path swept by the components of momentum transfer for fixed laboratory energy ( $T_{lab}=300$  MeV) and relative velocity as the integration needed to calculate the total elastic in-medium cross section is carried out. It is seen that it falls on the upper part of the zero sound branch for  $\hat{v}_y=0.41$  corresponding to the location of the peak in Fig. 2.

The lower branch of the zero sound falls in the particle-hole damping region. On the other hand, part of the upper branch falls outside the particle-hole damping zone where the imaginary part of  $D_{\sigma-\omega L}$  vanishes and corresponds to undamped modes at our level of approximation. This is at the origin of the narrowest peaks shown in Fig. 2, while the smoother peak is to be related to the lower branch for which particle/hole damping is active.

The zero-sound branches become more important as the density increases above a threshold value, their importance is reduced as temperature increases. It is indeed to be seen in Fig. 2a that the peak structure begins to develop above  $n = 0.5 n_0$  and in Fig. 2b that it is washed out at high temperature.

The size of the zero sound branch depends on the parameters, in particular on the cutoffs  $\Lambda_\sigma$  and  $\Lambda_\omega$ . However, even if these branches would disappear completely (by applying very low cutoffs), there would still be a strong reduction of the dispersion relation  $D_{\sigma-\omega L}(\omega, q)$  in this zone due to  $\sigma - \omega$  mixing and consequently an enhancement in the cross section. We believe that this broad enhancement at finite relative velocity matters more than the presence of a high but narrow peak. Its location will remain the same, coinciding with the upper limit of the particle hole damping zone.

## 5 Conclusion

In a relativistic OBE model of the N-N interaction with  $\sigma$ ,  $\omega$  and  $\pi$  meson exchange, we investigated the observable consequences of a modification of the elastic proton-proton cross section inside symmetric nuclear matter by screening of the interaction, *i.e.* by approximating the meson propagators at the RPA level.

It was found that the cross section is reduced when density increases and that the temperature and velocity dependence are non monotonous. For moderate values of the velocity, the cross section is enhanced at low densities and reduced at high densities if the velocity is inside the reaction plane ( $y, z$ ) and no appreciable modification is observed for velocities orthogonal to the reaction plane ( $v//x$ ). When the fluid flows inside the reaction plane, a series of peaks appear for a characteristic value of the velocity  $\hat{v}$  fulfilling the resonance condition for the excitation of zero sound. This collective mode appears in the mixed  $\sigma - \omega$  longitudinal part of the dispersion relation of the meson propagator which mediates the interaction. This occurs in the ultrarelativistic range when the fluid flows parallel to the direction of the incident particles ( $v//z$ ). On the other hand, if  $v//y$  the peaks occur at physically relevant values  $0.3 < \hat{v}_y < 0.8$ . Their location is density dependent; the peaks are stronger at higher density and gradually blur out when increasing temperature.

The angular dependence of the differential cross section deviates appreciably from the vacuum result. High densities favor forward/backward peaking. Finite velocities also contribute to make the cross section more forward/backward peaked with respect to the vacuum value and to the value in the case where the fluid is at rest.

The main result of our calculations is the enhancement introduced by the excitation of the zero sound modes of the medium on both the differential and the total elastic cross sections. It occurs for  $v//y$  but not for  $v//x$  or for unrealistic values of  $v//z$ . This strongly asymmetric situation might lead to observable consequences for the angular distribution of secondary particles in heavy ion collisions at intermediate energy and should be taken into account in the numerical analysis of the experimental results. In a naive hydrodynamical picture where the colliding particles fly along the beam axis whereas the background matter is approximated as a radially expanding fireball, the condition for sizeable enhancement of the cross section predicted by our model would be fulfilled in two caps on either side of the beam axis. We think it could be worthwhile to investigate this point in a refined kinetic simulation.

## References



- [1] D.T. Khoa, N. Ohtsuka, M.A. Marin, A. Faessler, S.W. Huang, E. Lehman, R. Puri, Nucl. Phys. **A548** (1992) 102.
- [2] E.I. Tanaka, A. Ono, H. Horiuchi, T. Maruyama and E. Engel, Phys. Rev. **C52** (1995) 316.
- [3] G.D. Westfall *et al.*, Phys. Rev. Lett. **71** (1993) 1986; V. de la Mota *et al.*, Phys. Rev. **C46** (1992) 677; B.A. Li, Phys. Rev. **C48** (1993) 2415.
- [4] D. Klakow, G. Welke and W. Bauer, Phys. Rev. **C48** (1993) 1982.
- [5] see *e.g.* R.B. Clare and D. Strottman, Phys. Rep. **141** (1986) 177; H.H.K. Tang and C.Y. Wong, Phys. Rev. **C21** (1980) 1846, *ibid* **C26** (1982) 284; W. Schmidt, B. Waldhauser, H. Stöcker, J.A. Maruhn, W. Greiner, Phys. Rev. **C47** (1993) 2782.
- [6] J. Cugnon, T. Mizutani and J. Vandermeulen, Phys. Rev. **C48** (1981) 505.
- [7] A. Bohnet, N. Ohtsuka, J. Aichelin, R. Linden and A. Faessler, Nucl. Phys. **A494** (1989) 349; A. Faessler, Nucl. Phys. **A495** (1989) 103c.
- [8] C. Fuchs, L. Sehn and H.H. Wolter, Nucl. Phys. **A601** (1996) 505.
- [9] G.Q. Li and R. Machleidt, Phys. Rev. **C48** (1993) 1702.
- [10] T. Alm, G. Röpke, W. Bauer, F. Daffin, M. Schmidt, Nucl. Phys. **A587** (1995) 815; T. Alm, G. Röpke, M. Schmidt, Phys. Rev. **C50** (1994) 31.
- [11] B. ter Haar and R. Malfliet, Phys. Rev. **C36** (1987) 1611.
- [12] J. Diaz-Alonso, L. Mornas, “*Screening effects on the elastic nucleon-nucleon cross-section in relativistic nuclear matter*”, to appear in Nucl. Phys. A
- [13] B.D. Serot, J.D. Walecka, “*The Relativistic Nuclear Many-Body Problem*”, Adv. Nucl. Phys., **16**, J.W. Negele and E. Vogt Edts. (Plenum, New York, 1986)
- [14] Nijmegen NN-Online Database described in V.G.J Stoks *et al.* Phys. Rev. **C47**, (1993), 761, *ibid.* **C48** (1993) 792 and SAID program by R.A. Arndt *et al.* Phys. Rev. **C50**, 2731 (1994).
- [15] J. Diaz Alonso and A. Pérez Canyellas, Nucl. Phys. **A526** (1991) 623.
- [16] E. Gallego, J. Diaz Alonso and A. Pérez, Nucl. Phys. **A578** (1994) 542; J. Diaz Alonso, E. Gallego and A. Perez, Phys. Rev. Lett. **73** (1994) 2536.
- [17] J. Diaz Alonso, B. Friman, P.A. Henning, “*Normal Modes in Nuclear Matter at Finite Temperature*”. Unpublished preprint G.S.I. Darmstadt (1992). Some results of this last reference have been published in P.A. Henning, Phys. Rep. **253** (1995), 235.
- [18] D. Krofcheck *et al.*, Phys. Rev. Lett. **63** (1989) 2028.
- [19] E.I. Tanaka, H. Horiuchi and A. Ono, “*Determination of in-medium nucleon-nucleon cross section from the data of proton-induced reaction cross-section*”, preprint Kyoto Univ. KUNS-1364 (1996)

### Figure captions

**Fig. 1:** Total elastic pp cross section as a function of the beam energy for various values of the density and temperature, vanishing relative velocity.

**Fig. 2:** Ratio of the in-medium cross section with respect to its value in the vacuum  $\sigma_{med}/\sigma_{free}$  as a function of velocity  $(0, v_y, 0)$ . — (a) for density  $n/n_0 = 0.1, 0.5, 1, 2, 5$  — (b) temperature dependence at  $n = n_0$ .

**Fig. 3:** Levels of constant value of the mixed  $\sigma$ –longitudinal  $\omega$  dispersion relation  $D_{\sigma-\omega L}(\omega, q)$  in the  $q - \omega$  plane of transferred momentum. The long-dashed line  $\hat{v}_y = 0.41$  corresponds to the resonant condition  $\hat{\gamma}_y \hat{v}_y p \sin \theta = \omega_{zs}$ .

**Fig. 1**

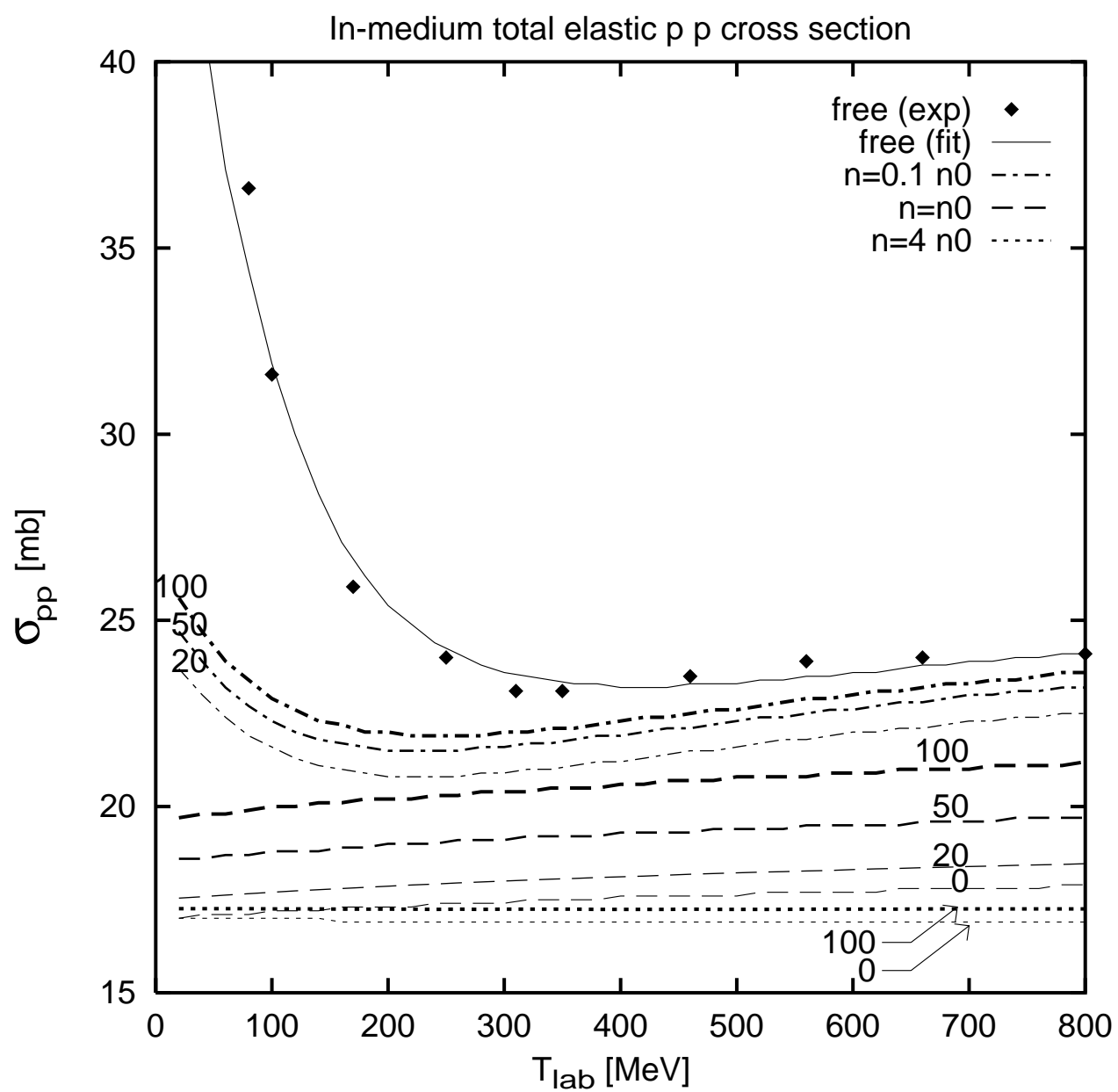


**Fig. 2a**

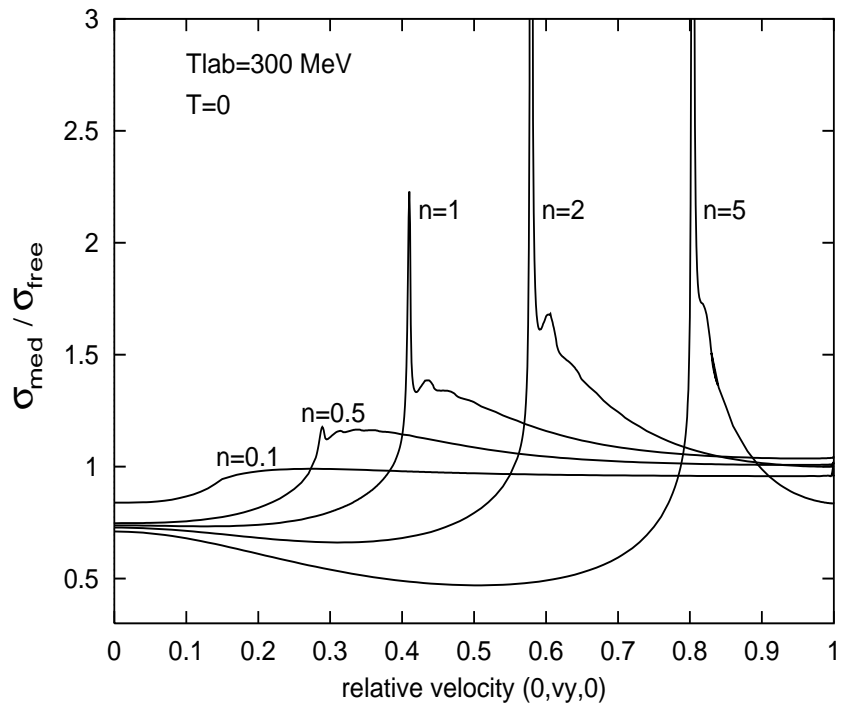


**Fig. 2b**

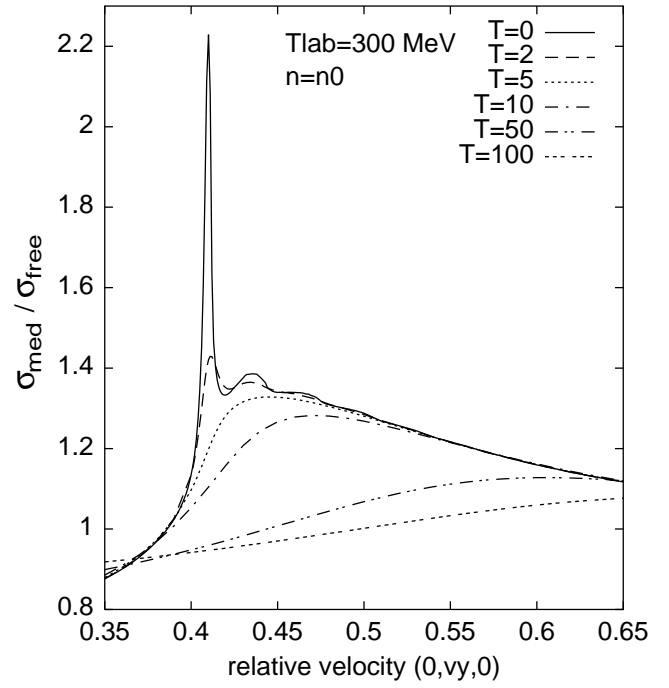


**Fig. 3**

